Seismic facies analysis using generative topographic mapping

Satinder Chopra⁺ and Kurt J. Marfurt†*
⁺Arcis Seismic Solutions, Calgary; †The University of Oklahoma, Norman

Summary

Seismic facies analysis is commonly carried out by classifying seismic waveforms based on their shapes in an interval of interest. It is also carried out by using different seismic attributes, reducing the dimensionality of the input data volumes using Kohonen's self-organizing maps (SOM), and organizing it into clusters on a 2D map. Such methods are computationally fast and inexpensive. However, they have shortcomings in that there is no definite criteria for selection of a search radius and the learning rate, as these are parameters dependent on the input data. In addition, there is no cost function that is defined and optimized and so usually the method is deficient in providing a measure of confidence that could be assigned to the results.

Generative topographic mapping (GTM) has been shown to address the shortcomings of the SOM method and suggested as an alternative to it. We demonstrate the application of GTM to a dataset from central Alberta, Canada and show that its performance is more encouraging than the simplistic waveform classification or the SOM multiattribute approach.

Introduction

The shape and character of the seismic waveform is often used to characterize reservoir quality. Such a seismic waveform carries information about the phase, frequency and amplitude; any variation in these parameters is a function of the lateral variations in lithology, porosity and fluid content. If the shape and character of seismic waveforms in a given target zone can be studied using some pattern recognition type of a process and then displayed in a map view, the display would indicate seismic facies variation at the target level.

One approach to pattern recognition is with the use of neural networks to compare seismic waveforms within the interval of interest with a series of synthetic traces. These synthetic traces are generated according to the user-defined number of groups that best represent the different shapes in the interval. They are arranged in a progression (assigning numbers to these traces), which is examined to get a feel for the shapes of the waveforms. Next, each trace in the interval is compared with the different synthetic traces and those traces that have maximum correlation with a given synthetic trace are classified into a group. The resulting map is essentially a facies map, or a similarity map of the actual traces to the different synthetic traces. The seismic facies so generated also can be overlaid on a vertical seismic section to study their lateral variation. Since this method does not require any input in the form of any well log or any guidance about where the character divisions should occur, this approach is referred to as *unsupervised* waveform classification. We apply this classification to a 3D seismic volume from central Alberta, Canada, where we focus on the Mannville channels at a depth of 1150 to 1230 m that are filled with interbedded units of shale and sandstone. On the 3D seismic volume, these channels show up at a mean time of 1000 ms plus or minus 50 ms. In Figure 1 we show a segment of a vertical slice through the seismic amplitude data, which shows differential compaction within the channels, indicated with yellow arrows. The 11 waveforms are shown in Figure 1c. Note that each waveform is very similar to the one to its left and right, but quite different from those far away. The seismic facies distribution is computed by cross-correlating these seismic waveforms with the windowed data. The colors in the waveform classification map in Figure 1b correspond to the waveform with the highest cross-correlation coefficient. Note that the channel fill within the main channel to the left is different from the other features on the display. Some of the colored patches are seen on the lower and upper right side of the display. These patches could be further subdivided into more detail, but is not attempted here.

The self-organizing maps (SOM) waveform classification algorithm that produced the 2D seismic facies display in Figure 1b was introduced by Kohonen (1982, 2001) in speech recognition work. This work was subsequently applied to seismic data by Poupon et al. (1999), Strecker and Uden (2002), and Coleou et al. (2003). Essentially, the 16-sample vertical waveforms in an analysis time window are projected into a 1D manifold lying in 16-dimensional space, which is then displayed using a 1D color bar. Attempts have been made to extend such analysis into 2D or 3D subspace. Using seismic attributes such as amplitude envelope, bandwidth, impedance, AVO slope and intercept, dip magnitude and coherence, Strecker and Uden (2002) projected them into 2D latent space and plotted the results with a 2D color bar.

Roy et al. (2012) used 3D SOM multiattribute application to generate a 3D seismic facies volume. The different

DOI http://dx.doi.org/10.1190/segam2014-0233.1

mathematically independent input attributes determine the dimensionality of the latent space. The input data vectors are first normalized and then projected into the 2D latent space using principal component analysis in the form of eigenvalues and eigenvectors. As part of the training process, each vector is chosen at random and compared to all the other vectors on the 2D latent space grid in a neighborhood radius and the vectors with good correlation are updated. Next, smaller neighborhoods around the correlated vectors are also updated, and gradually the neighborhood radius is shrunk iteratively. If there are five attributes and we are using a 2D latent space, the initial PCA plane is deformed into a 2D nonplanar manifold (or surface) in 5D space that best fits the data. Colors are assigned to the vectors according to their distance from the center of a given cluster of points. In this way a 3D volume of facies is generated.

The method

The Kohonen self-organizing map described above, while the most popular unsupervised clustering technique, being easy to implement and computationally inexpensive, has limitations. There is no theoretical basis for selecting the training radius, neighborhood function and learning rate as these parameters are data dependent (Bishop et al., 1998; Roy, 2013). No cost function is defined that could be iteratively minimized and would indicate the convergence of the iterations during the training process, and finally no probability density is defined that could yield a confidence measure in the final clustering results. Bishop et al. (1998) developed an alternative approach to the Kohonen self-organizing map approach that overcomes its limitations. It is called generative topographic mapping (GTM) algorithm, and is a nonlinear dimension reduction technique that provides a probabilistic representation of the data vectors in latent space.

The GTM method begins with an initial array of grid points arranged on a lower dimensional latent space. Each of the grid points are then nonlinearly mapped onto a similar dimensional non-Euclidean curved surface as a corresponding vector ($\mathbf{m_k}$) embedded into different dimensional data space in GTM. Each data vector ($\mathbf{x_k}$) mapped into this space is modeled as a suite of Gaussian probability density functions centered on these reference vectors ($\mathbf{m_k}$). The components of the Gaussian model are then iteratively made to move toward the data vector that it best represents. Roy (2013) and Roy et al. (2014) describe the details of the method and demonstrate its application for mapping of seismic facies to the Veracruz Basin, Mexico.

We applied GTM to the same data shown in Figure 1, and using the sweetness, GLCM-energy, GLCM-entropy, GLCM-homogeneity, peak frequency, peak magnitude, coherence and impedance attributes and derived GTM1 and GTM2 outputs. These attributes provide the cluster locations (projection of the mean posterior probability of the data vectors) along the two axes in the latent space to be used in the crossplotting that follows. In Figure 2a we show a coherence stratal slice distinctively exhibiting the different channels. In Figures 2b and c we show the equivalent displays for GTM 1 and GTM2 attributes. Breaking the 2D latent space into two components allows us to use modern interactive crossplotting tools. Notice, while GTM1 shows the definition of the edges very well for the channels, GTM2 exhibits the complete definition of the channels along with their fill in red and blue. In a narrow zone passing through the center of the channels we crossplot the two attributes GTM1 and GTM2 and then by assigning red and green polygons on two clusters (not shown) we notice how the enclosed points are projected back on the coherence displays shown in Figure 3. The two clusters highlight the fill of the channels differently.

More work is underway to bring constraints into this unconstrained GTM classification, by using well log data, as has been demonstrated by Roy et al. (2013).

Conclusions

While Kohonen SOM is a popular method used for unconstrained seismic amplitude and attribute classification, it has limitations as mentioned above. GTM analysis provides an alternative approach by way of nonlinear dimension reduction in latent space, and providing probabilistic representation of the data. The application of the GTM analysis to a dataset from central Alberta, Canada shows encouraging results. We expect that by using constrained GTM analysis with the help of well log data, the facies patterns we have derived using the unconstrained GTM method used here would be further tightened and made more distinct.

Acknowledgements

We wish to thank Arcis Seismic Solutions, TGS for encouraging this work and for permission to present these results.

DOI http://dx.doi.org/10.1190/segam2014-0233.1

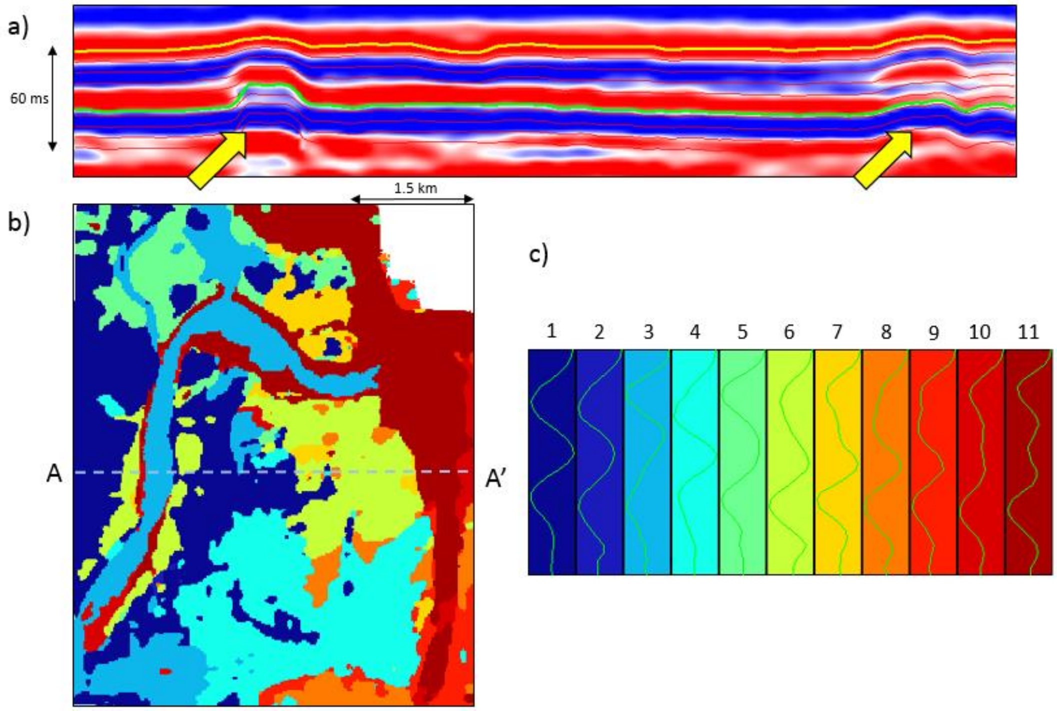

Figure 1: (a) Vertical slice through a seismic amplitude volume showing the interval that was chosen for waveform classification, (b) waveform classification map showing the features in different colors, and (c) the eleven different waveforms used in the waveform classification map shown in (b). Yellow arrows indicate two channels that have experienced less differential compaction than the surrounding flood plane. These two channels have radically different waveforms (one indigo, one reddish brown).

DOI http://dx.doi.org/10.1190/segam2014-0233.1

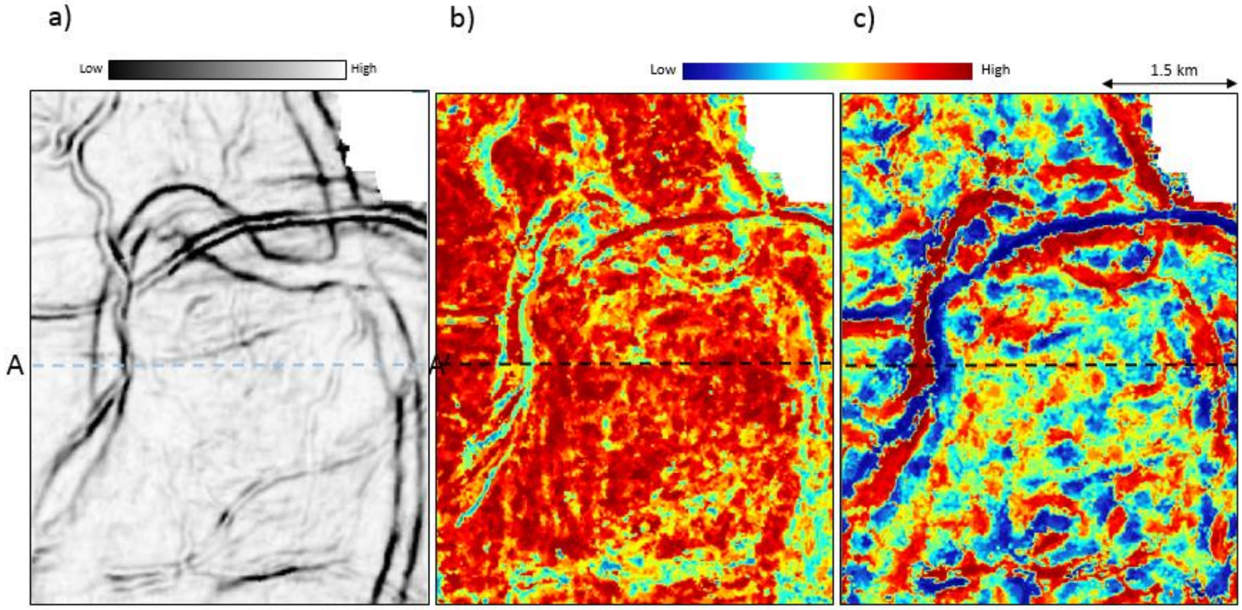

Figure 2: Stratal-slice close to the green horizon shown in the previous image through (a) energy ratio coherence, (b) GTM component 1 and (c) GTM component 2.

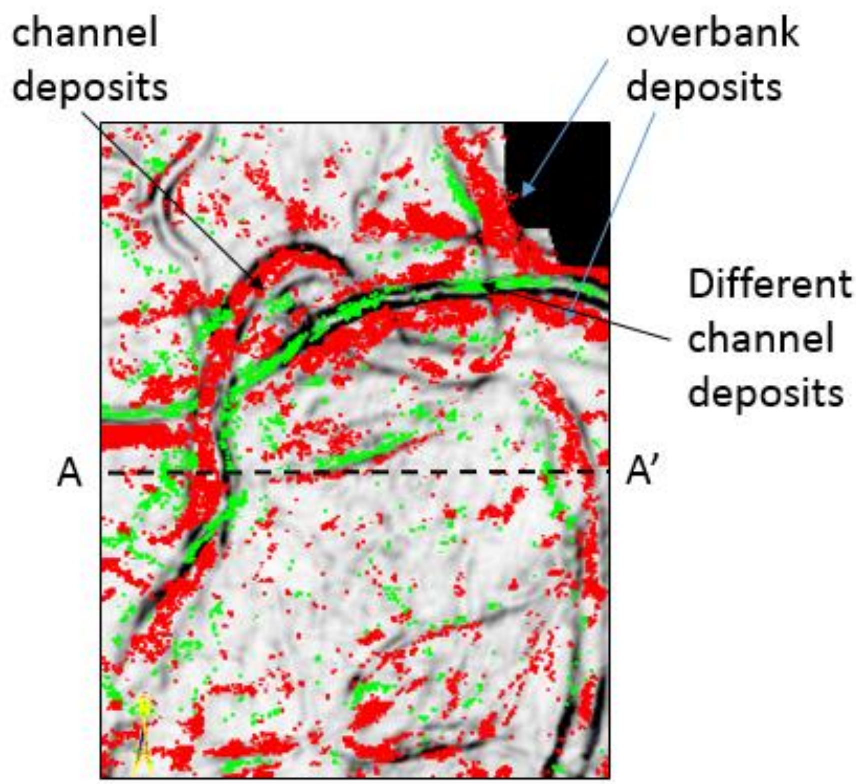

Figure 3: Two interpreter selected clusters (one red, one green) selected by drawing polygons in GTM1 vs. GTM2 crossplot histogram co-rendered onto a coherence background. Note the two channels fall into different clusters indicating different thicknesses and or lithologies. Note that the infill of the two channels seen in Figure 1a both appear to be in the same red class in this image.

DOI http://dx.doi.org/10.1190/segam2014-0233.1

http://dx.doi.org/10.1190/segam2014-0233.1

EDITED REFERENCES

Note: This reference list is a copy-edited version of the reference list submitted by the author. Reference lists for the 2014 SEG Technical Program Expanded Abstracts have been copy edited so that references provided with the online metadata for each paper will achieve a high degree of linking to cited sources that appear on the Web.

REFERENCES

Bishop, C. M., M. Svensén, and C. K. I. Williams, 1998, GTM: The generative topographic mapping: Neural Computation, **10**, no. 1, 215–234, http://dx.doi.org/10.1162/089976698300017953.

Coléou, T., M. Poupon, and K. Azbel, 2003, Unsupervised seismic facies classification: A review and comparison of techniques and implementation: The Leading Edge, **22**, 942–953, http://dx.doi.org/10.1190/1.1623635.

Kohonen, T., 1982, Self-organized formation of topologically correct feature maps: Biological Cybernetics, **43**, no. 1, 59–69, http://dx.doi.org/10.1007/BF00337288.

Kohonen, T., 2001, Self-organizing maps, 3rd ed.: Springer.

Poupon, M., K. Azbel, and G. Palmer, 1999, A new methodology based on seismic facies analysis and litho-seismic modeling: The Elkhorn Slough field pilot project, Solano County, California: 69th Annual International Meeting, SEG, Expanded Abstracts, 927–930.

Roy, A., 2013, Latent space classification of seismic facies: Ph.D. dissertation, University of Oklahoma.

Roy, A., B. L. Dowel, and K. J. Marfurt, 2012, Characterizing a Mississippian tripolitic chert reservoir using 3D unsupervised seismic facies analysis and well logs: An example from Osage County, Oklahoma: 82nd Annual International Meeting, SEG, Expanded Abstracts, doi: 10.1190/segam2012-1365.1.

Roy, A., A. S. Romero-Peláez, T. J. Kwiatkowski, and K. Marfurt, 2014, Generative topographic mapping for seismic facies estimation of a carbonate wash, Veracruz Basin, southern Mexico: Interpretation, **2**, no. 1, SA31–SA47, http://dx.doi.org/10.1190/INT-2013-0077.1.

Strecker, U., and R. Uden, 2002, Data mining of 3D post-stack seismic attribute volumes using Kohonen self-organizing maps: The Leading Edge, **21**, 1032–1037, http://dx.doi.org/10.1190/1.1518442.